

# Experimental study and analytical modeling of preferential flow and partitioning dynamics at unsaturated fracture intersections

Torsten Noffz<sup>1</sup>, Marco Dentz<sup>2</sup>, and Jannes Kordilla<sup>1</sup>

<sup>1</sup>University of Göttingen, Geoscientific Centre (GZG), Göttingen, Germany

<sup>2</sup>Institute of Environmental Assessment and Water Research (IDAEA), Spanish National Research Council (CSIC), Barcelona, Spain

November 21, 2022

## Abstract

Unsaturated fractured aquifer systems offer a domain for complex gravity-driven flow dynamics leading to the development of preferential flow along fracture networks that often strongly contributes to rapid mass fluxes. This behaviour is difficult to recover by volume-effective modeling approaches (e.g. Richards equation) due to the non-linear nature of free-surface flows and mass partitioning processes at unsaturated fracture intersections. The application of well-controlled laboratory experiments enables to isolate single aspects of the mass redistribution process that ultimately affects travel time distributions across scales. We use custom-made acrylic cubes (20 cm x 20 cm x 20 cm) in analogue percolation experiments to create simple fracture networks with single or multiple horizontal fractures. A high precision multichannel dispenser produces gravity-driven free surface flow (droplets; rivulets) at flow rates ranging from 1 ml/min to 5 ml/min. Hereby, total inflow rates are kept constant while the fluid is injected via 15 (droplet flow) or 3 inlets (rivulet flow) to reduce the impact of erratic flow dynamics. Normalized fracture inflow rates ( $Q_f/Q_0$ ) are calculated and compared for aperture widths  $d_f$  of 1 mm and 2.5 mm. A higher efficiency in filling an unsaturated fracture by rivulet flow observed in former studies can be confirmed. The onset of a capillary driven Washburn-type flow is determined and recovered by an analytical solution. In order to upscale the dynamics and enable the prediction of mass partitioning for arbitrary-sized fracture cascades a Gaussian transfer function is derived that reproduces the repetitive filling of fractures, where rivulet flow is the prevailing regime. Results show good agreement with experimental data for all tested aperture widths.

# Experimental study and analytical modeling of preferential flow and partitioning dynamics at unsaturated fracture intersections

## I. Introduction

## II. Methods (cont.)

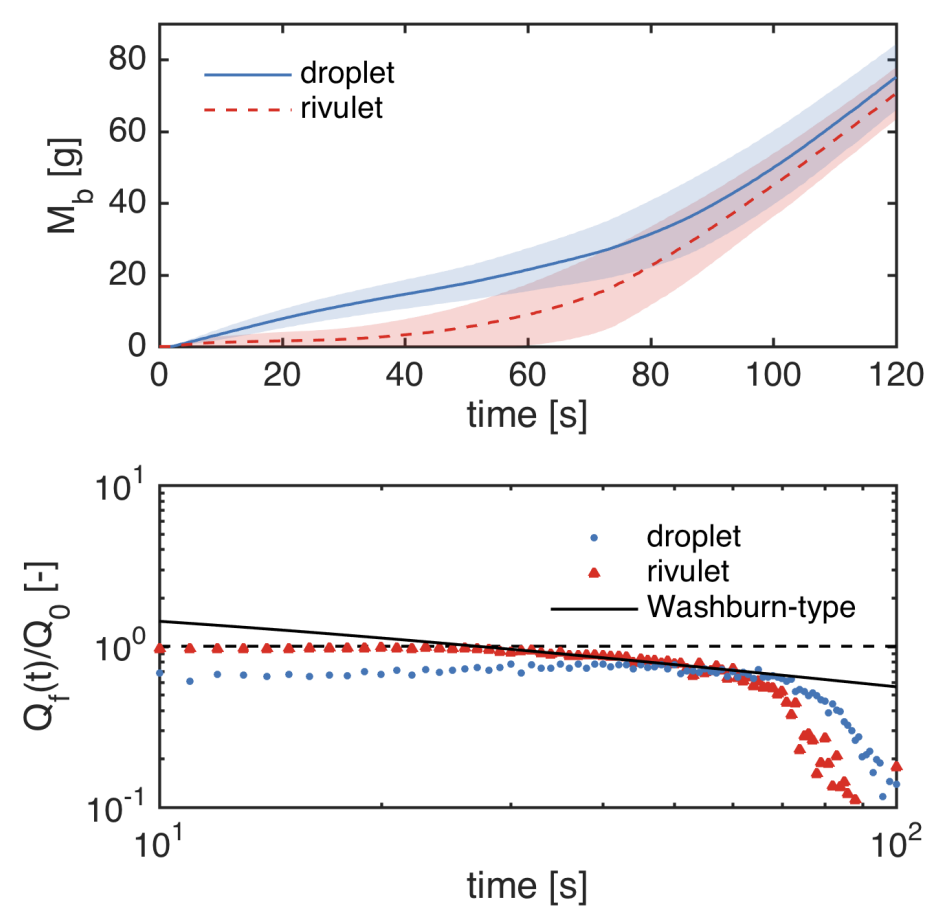
## III. Results & Discussion (cont.)

### 1. Unsaturated flow

- Complex, gravity-driven flow dynamics in macropores of soils (Nimmo, 2012) and along fracture networks (Dahan et al. 1999, 2000; Kordilla et al., 2017) or fault zones (Bodvarsson et al., 1997; Liu et al., 2004) may lead to the formation of preferential flow paths in the vadose zone triggering rapid mass fluxes
- The non-linear nature of free-surface flow and mass partitioning processes at fracture intersections may be difficult to recover by volume-effective modelling approaches (e.g. Richards' equation) and unified conceptual frameworks do not exist (Ghezzehei, 2004)

### 2. Analogue experiments

- Well controlled analogue percolation experiments may aid to investigate the formation of flow modes and instabilities (Jones et al., 2018; Li et al., 2018) and the role of unsaturated fracture intersections on mass partitioning processes (e.g., Ji et al., 2006; Kordilla et al., 2017; LaViolette et al., 2003; Nicholl and Glass, 2005; Wood et al., 2002, 2005; Wood and Huang, 2015)
- These studies highlight the importance of fracture intersections Figure 1: Accumulated mass  $M_b$  as capillary barriers, which may induce pulsating flows and act as anas integrators for dispersion and recharge processes (Kordilla et al., 2017).



### 3. Objective

- Confirm strong contrast in the bypass efficiency of droplet and rivulet flow observed in former experiments (Kordilla et al., 2017)
- Test an analytical solution for capillary-driven fracture inflow proposed by Kordilla et al. (2017)
- Apply a transfer-function approach for predictive modelling of mass partitioning processes at unsaturated fracture intersections of arbitrary-sized fracture cascades (Jury, 1986; Noffz et al., 2018)

## II. Methods

### 1. Experimental approach

- The analogue fracture network consists of two to four vertically stacked poly(methyl methacrylate) (PMMA) cubes (20 cm × 20 cm × 20 cm)
- Aperture width  $d_f$  is either 1 mm or 2.5 mm
- The non-porous substrate exhibits a static contact angle  $\theta_0$  of  $65.2 \pm 2.9^\circ$
- Two injection methods are tested while the total volumetric flow rate  $Q_0$  is  $15 \text{ ml min}^{-1}$ :

- 1  $15 \times 1 \text{ ml min}^{-1}$  (droplet flow)
- 2  $3 \times 5 \text{ ml min}^{-1}$  (rivulet flow)



Figure 2: Injection methods used in analogue percolation experiments.

### 2. Mass partitioning

- The total injected mass  $M$  at time  $t$  is

$$M(t) = Q_0 t \quad (1)$$

- Its redistribution at the unsaturated fracture intersection is given by

$$M(t) = M_f(t) + M_1(t) \quad (2)$$

- Here,  $M_f$  is the mass in the fracture and  $M_1$  the mass accumulated on the drip pan. Derivation of Eq. (2) gives

$$\frac{dM(t)}{dt} = Q_0 = \frac{dM_f(t)}{dt} + \frac{dM_1(t)}{dt} \quad (3)$$

- Hence, the volumetric fracture inflow rate  $Q_f [L^3 T^{-1}]$  is

$$Q_f(t) = \frac{dM_f(t)}{dt} = Q_0 - Q_1(t) \quad (4)$$

### 3. Washburn-type fracture inflow

- An analytical solution for capillary driven fracture inflow  $Q_f$  following Washburn (1921) and Bell & Cameron (1905) is proposed by Kordilla et al. (2017). Penetration length  $l(t)$  is obtained by

$$\frac{dl(t)}{dt} = \frac{d_f^2 \Delta P_c}{4\eta l(t)} \quad (5)$$

- Here,  $\eta$  is viscosity and  $\Delta P_c$  capillary pressure. For the initial length (i.e.  $l(t = t_0) = l_0$ ) Eq. (5) gives

$$l(t) = l_0 \sqrt{1 + \frac{d_f^2 \Delta P_c}{2\eta l_0^2} (t - t_0)} \quad (6)$$

- The fluid mass within the fracture is  $M_f(t) = A_f l(t) \rho_w$ , where  $\rho_w$  accounts for water density and  $A_f$  for the cross-sectional fracture area

- Here,  $\varphi_{n_f}(t)$  is the transfer function that accounts for vertical film flow and flow partitioning in cube  $n$ . For a single fracture the relation is

$$Q_1(t) = Q_0 \int_0^t dt' \varphi(t') \quad (9)$$

## III. Results & Discussion

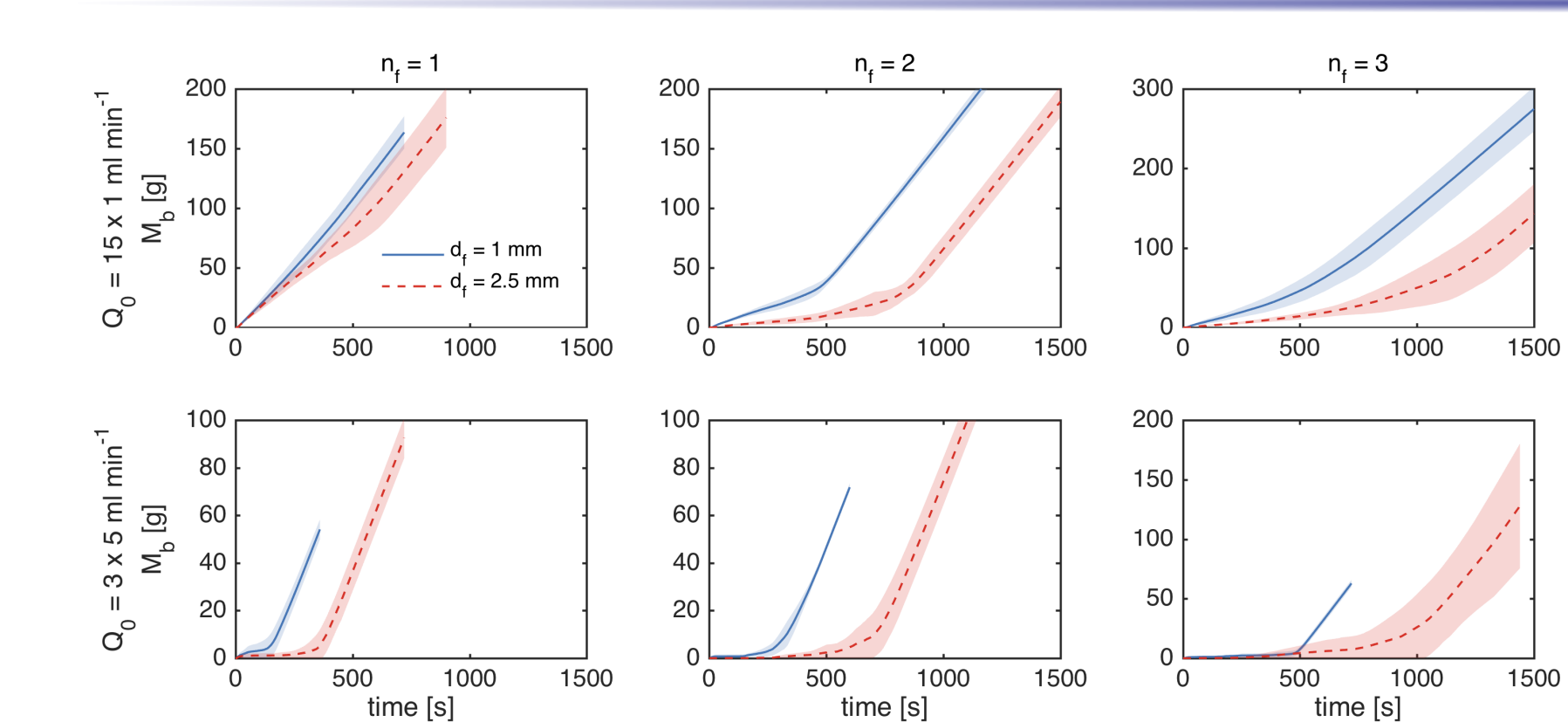


Figure 4: Accumulated mass  $M_b$  vs. time for droplet (top) and rivulet (bottom) produced by a multi-inlet array. From Noffz et al. (2018).

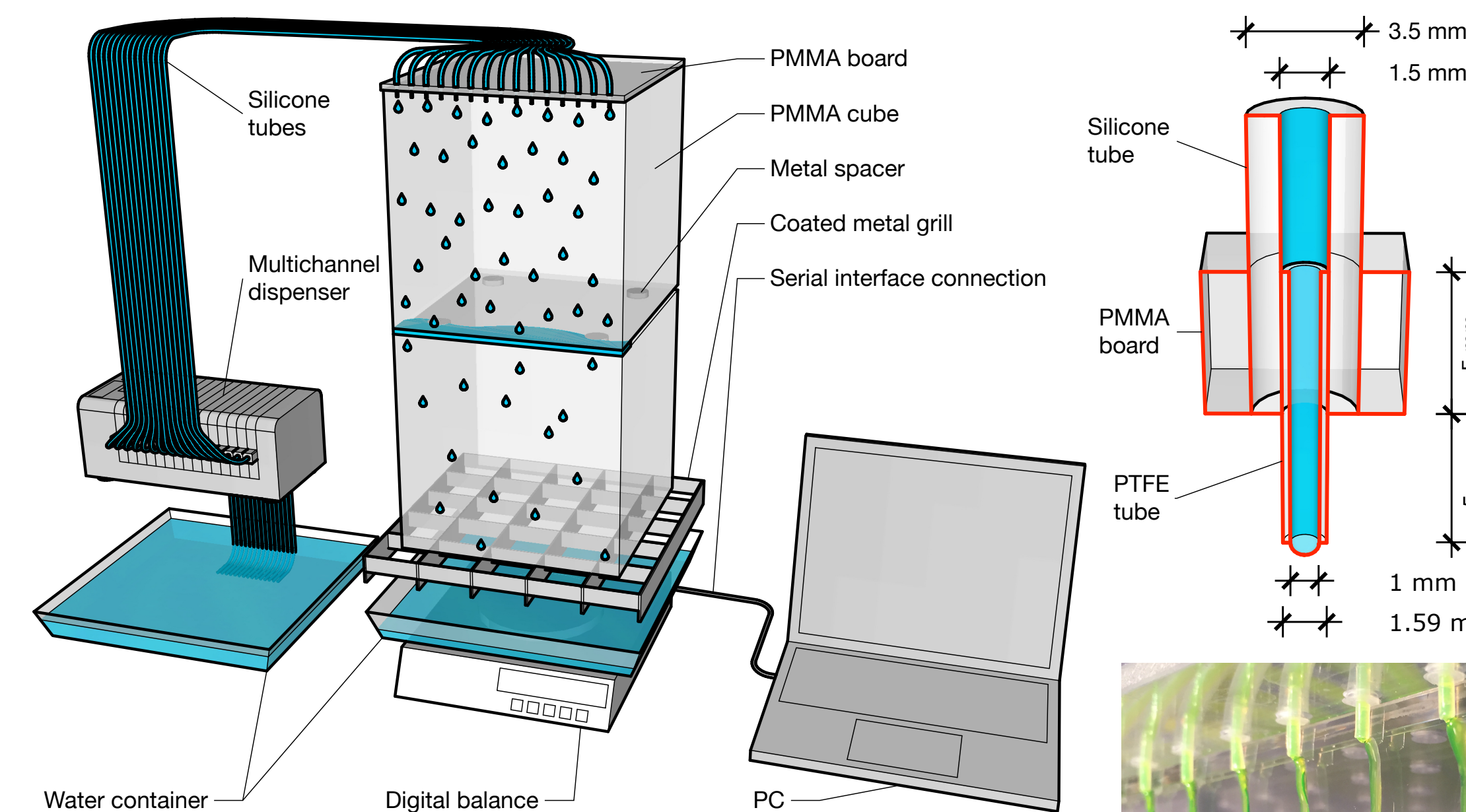


Figure 3: Sketch of laboratory setup (left) and injection nozzle (right). From Noffz et al. (2018).

- The flow rate into the fracture according to Eq. (4) becomes

$$Q_f(t) = \frac{Q_0}{\sqrt{1 + 2k_f(t - t_0)}} \quad (7)$$

- The transition constant is defined as  $k_f = \frac{d_f^2 \Delta P_c}{2\eta l_0^2}$

### 4. Transfer function

- The outflow rate at the bottom of the network is considered in the context of transfer function theory (Jury, 1986)
- The output signal  $Q_{n+1}(t)$  at the bottom of cube  $n$  is given in terms of the input signal  $Q_n(t)$  at the top as

$$Q_{n_f}(t) = \int_0^t \varphi_{n_f}(t - t') Q_{n_f-1}(t') \quad (8)$$

- Here,  $\varphi_{n_f}(t)$  is the transfer function that accounts for vertical film flow and flow partitioning in cube  $n$ . For a single fracture the relation is

- The transfer function is characteristic of the mass redistribution at the fracture intersection and relates to the flow rate at the drip pan and within the fracture as

$$\varphi(t) = \frac{dQ_1(t)}{dt} = -\frac{dQ_f(t)}{dt} \quad (10)$$

- For rivulet flow the transfer function may be estimated from the output signal at the bottom of the second cube according to Eq. (10)

- The transfer function is zero before the onset of the Washburn type flow  $t_0$  and reaches a maximum after which it decreases exponentially fast

- The truncated Gaussian is employed to capture these features

$$\varphi(t) \propto \frac{\exp\left[-\frac{(t-\mu)^2}{2\sigma^2}\right]}{\sqrt{2\pi\sigma^2}} \quad (11)$$

- Here,  $\mu$  denotes the mean and  $\sigma^2$  the variance

- Furthermore, the transfer function is normalized to 1, hence

$$\int_0^\infty dt \varphi(t) = 1 \quad (12)$$

- For the total fracture flow the approach gives  $Q_{f,n_f}$  after  $n_f$  cubes

$$Q_{f,n_f}(t) = Q_0 \dots \quad (13)$$

$$\left[ 1 - \int_0^t dt_{n_f-1} \varphi(t - t_{n_f-1}) \dots \int_0^{t_3} dt_2 \varphi(t_3 - t_2) \int_0^{t_2} dt_1 \varphi(t_1) \right]$$

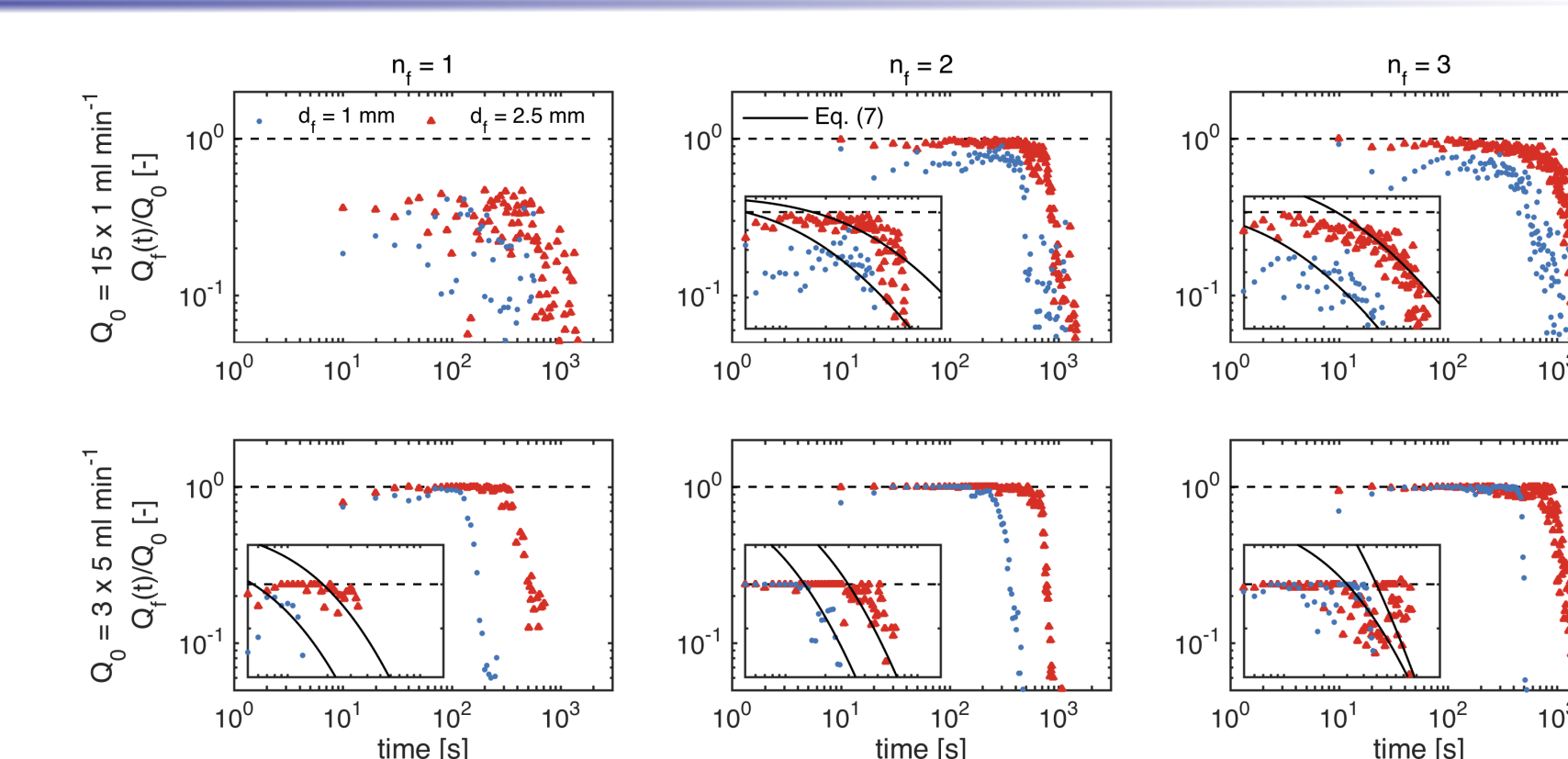


Figure 5: Adjusted parameters  $t_0$  and  $k_f$  for fitting of Eq. (7). From Noffz et al. (2018).

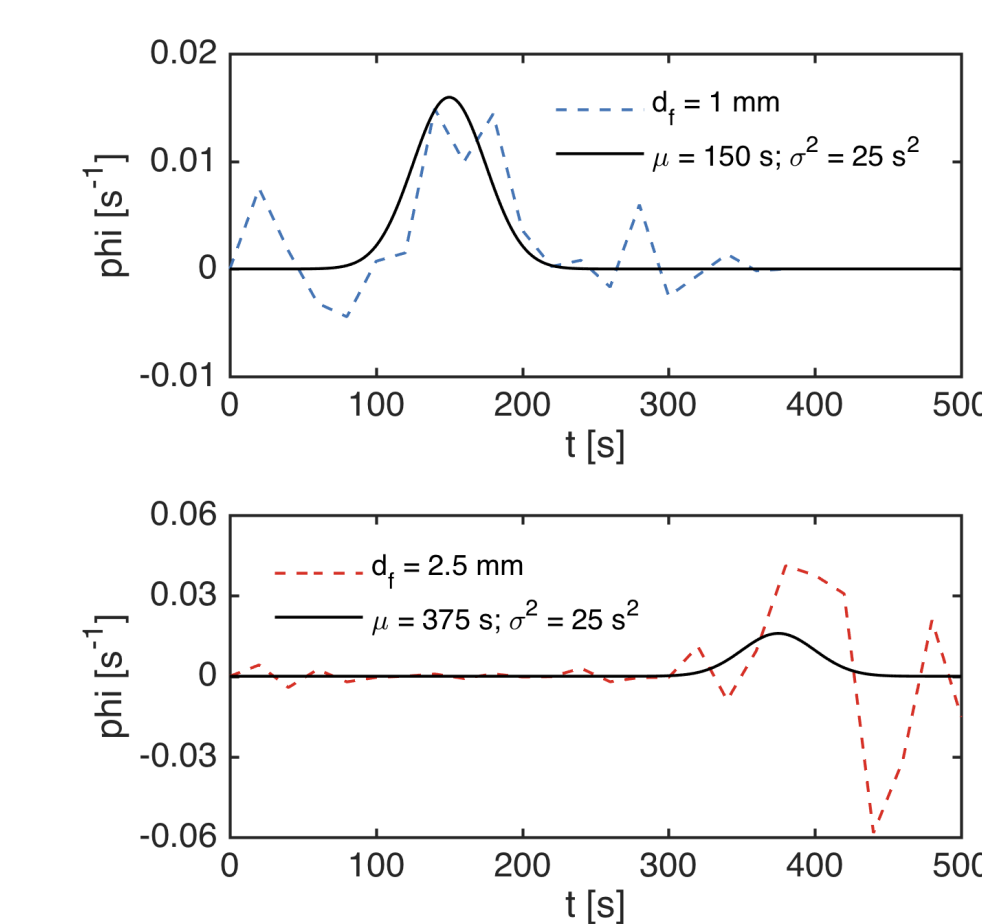


Figure 7: Transfer functions  $\varphi$  for rivulet flow at a single fracture intersection (dashed lines) and fitted Gaussian (solid lines). From Noffz et al. (2018).

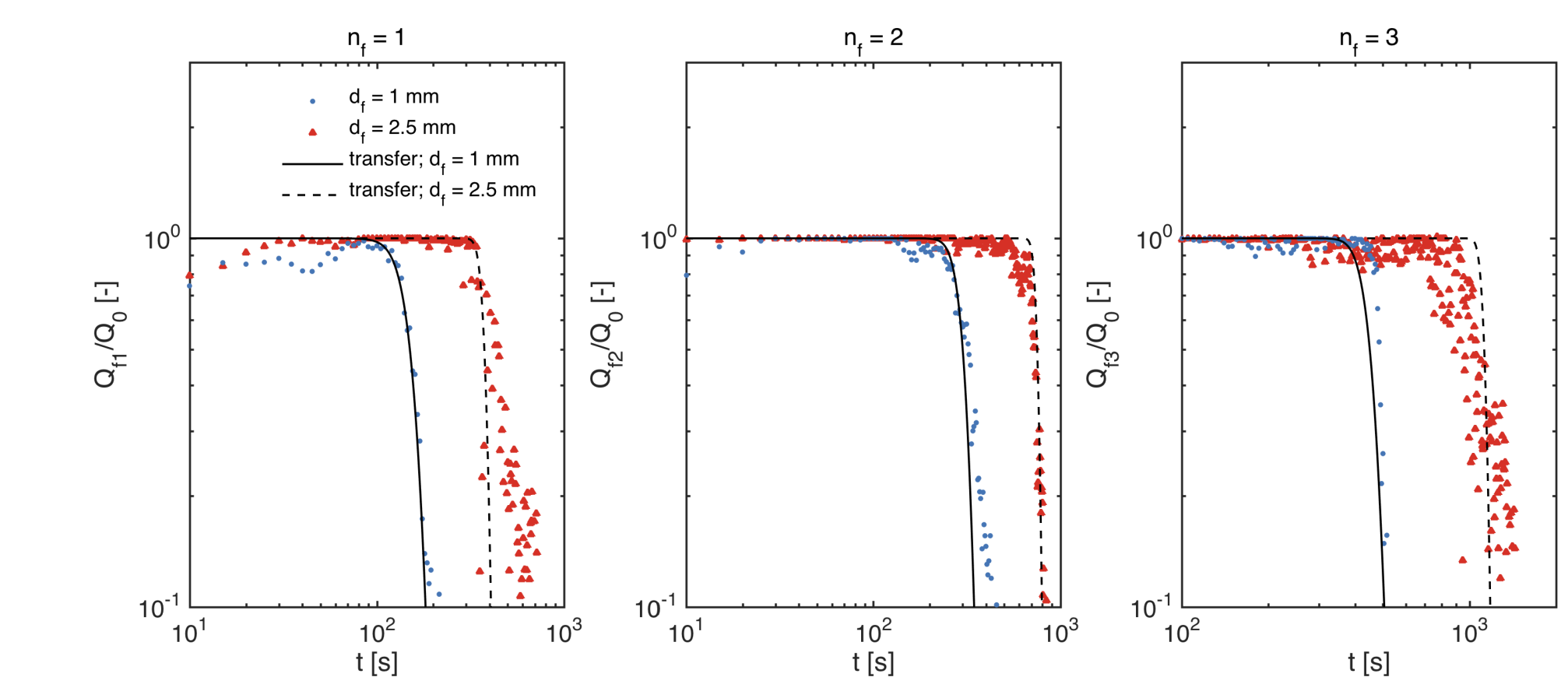


Figure 8: Normalized fracture inflow rates  $Q_f/Q_0$  during rivulet flow with predictions obtained by Eq. (13). From Noffz et al. (2018).

## IV. Conclusion

### 1. Mass redistribution at unsaturated fracture intersections

- A high bypass efficiency of droplet flow and the existence of a Washburn-type flow regime have been successfully presented in analogue percolation experiments
- The transfer function approach enables predictive modelling of mass partitioning dynamics during rivulet flow for arbitrary-sized fracture cascades (i.e.  $n_f \geq 1$ )

### 2. Limitations

- Tested fracture geometries are highly simplified and chosen materials do not account for the imbibition of a porous matrix

### 3. Outlook

- Further studies are required to investigate the impact of geometric features of natural fracture systems (e.g., roughness, aperture width, inclination) and material properties (e.g., wetting, contact angle dynamics, matrix-fracture interaction)

### Acknowledgements:

This work was funded by the Deutsche Forschungsgemeinschaft (DFG; German Research Foundation) under grant no. SA 501/26-1 and KO 53591/1-1. Marco Dentz acknowledges the funding from the European Research Council under the European Union's Seventh Framework Programme (FP7/2007-2013)/ ERC Grant Agreement No. 617511 (MHetScale).

### References:

Bell et al. (1905): J. of Phys. Chem. (10); Bodvarsson et al. (1997): Earth Sci. Div.; Dahan et al. (1999): Water Resour. Res. (35); Dahan et al. (2000): Groundwater (38); Ghezzehei (2004): Water Resour. Res. (40); Ji et al. (2006): Water Resour. Res. (42); Jones et al. (2018): Hydrogeol. J. (26); Jury (1986): Water Resour. Res. (22); Kordilla et al. (2017): Water Resour. Res. (53); LaViolette et al. (2003): Geophys. Res. L. (30); Li et al. (2018): Energies (11); Liu et al. (2004): J. of Cont. Hydrol. (74); Nicholl et al. (2005): Vad. Zone J. (4); Nimmo (2012): Hydr. Proc. (26); Noffz et al. (2018): Vad. Zone J.; Washburn (1921): Phys. Rev. (15); Wood et al. (2002): Geophys. Res. L. (29); Wood et al. (2005): Water Resour. Res. (41); Wood et al. (2015): Fl. Dyn. in Compl. Fract. Por. Sys.